IEEE Access
Multidisciplinary | Rapid Review | Open Access Journal

Received July 10, 2019, accepted July 31, 2019, date of publication August 5, 2019, date of current version August 19, 2019.

Digital Object Identifier 10.1109/ACCESS.2019.2933260

Modeling and Experimental Validation of a Butterfly-Shaped Wireless Power Transfer in Biomedical Implants

NAM HA-VAN[1], (Member, IEEE), AND CHULHUN SEO[2], (Senior Member, IEEE)
[1]Department of Information Communication, Materials, and Chemistry Convergence Technology, Soongsil University, Seoul 156-743, South Korea
[2]School of Electronic Engineering, Soongsil University, Seoul 156-743, South Korea

Corresponding author: Chulhun Seo (chulhun@ssu.ac.kr)

This work was supported by the National Research Foundation of Korea (NRF) Grant funded by the Korean Government (MSIP) (NRF-2017R1A5A1015596).

ABSTRACT Wireless power transfer (WPT) presents a safe and robust method for powering biomedical implants. The range and misalignment tolerance restrictions of the WPT system are the main factors, conducive to the transfer efficiency degradation. Especially, the implanted device is invisible and difficult to arrange in alignment with the transmitting coil. This paper proposes a butterfly-shaped transmitting (BS-Tx) coil of a magnetic resonance WPT system for biomedical implants. The BS-Tx coil prototypes with the changing driven current directions, parallel and anti-parallel current directions, are verified and analyzed. Besides, an equivalent circuit model of a coupling two-coil system with an optimal pair of capacitors method for the matching network is mathematically derived to obtain the maximized power transfer efficiency. The BS-Tx coil enhances the efficiency of the system in the distance, angle, and axial misalignment tolerances. A practical WPT system is fabricated and measured to verify the transfer efficiency through the real biological tissue and exhibits a significant efficiency improvement. Finally, a hypothetical context of retinal prosthesis application is demonstrated as a potential application to retinal implants. The proposed system shows a low specific absorption rate, that is satisfied the human safety regulations.

INDEX TERMS Biomedical implants, butterfly-shape, magnetic resonant, misalignment tolerance, retinal prosthesis, wireless power transfer.

I. INTRODUCTION

Wireless power transfer (WPT) system presents an emerging and promising way to provide a safe and convenient solution for the power supply of biomedical implants, which has attracted a lot of attention in recent years [1]–[5]. Beside the WPT techniques such as an inductive coupling system for very short distances of a few millimeters [6], [7], an electromagnetic wave system with the huge absorption rate in the human body [8]–[10], a magnetic resonance WPT system is one of the most suitable techniques for the implantable biomedical system [11]–[13]. However, the magnetic resonance WPT system still undergoes the efficiency reduction because of the changing receiving position in transfer distance, angle and axis misalignment. Especially, the implanted device is embedded under the tissue layer, which leads to the difficulty of determining the exact position of the receiving device. Besides, a large-sized implant increases the possibility of tissue inflammation, damage, and cell death [14]–[16]. The implant size should be minimized to reduce the risk of infection and increase the implant durability [17]. However, the miniaturization causes strong degradation of transfer efficiency. Therefore, the efficiency improvement is necessary for the biomedical implanted WPT system. A research is proposed to improve the WPT efficiency using a half-closed partially ceramic-filled cavity resonator [18], which can obtain high efficiency within the distance comparable to the diameter of the resonator. However, the angle and axial misalignment conditions are not considered to overcome the conventional WPT system restriction. Besides, a multi-coil-based WPT system in retinal implants is used to obtain high tolerance for compensation of coil misalignment effects on

The associate editor coordinating the review of this manuscript and approving it for publication was Tariq Masood.

the transfer efficiency and data bandwidth presented in [19]. Nevertheless, the multi-coil method was used to improve the coupling coefficient, which is suitable for the small coil misalignment range. In [20], a theory for tracking the optimal efficiency of the magnetic resonant WPT system was proposed to improve the efficiency despite variations in the distance, angle, and axial misalignment. However, the power transfer efficiency (PTE) of the biomedical implant WPT system is still low and insignificantly improved under varying conditions.

In this paper, a change of the transmitting (Tx) coil structure based on a butterfly shape is presented to overcome the efficiency degradation of a WPT system with variations in transfer distance, angle and axis misalignment. The butterfly-shaped transmitting (BS-Tx) coil is supplied by a single power source without any phase and current control methodology, which is simple to implement and fabricate the system. By changing the transmitting structure geometry, the magnetic field is modified to create a significantly strong field in the misalignment conditions. In [21], a BS-Tx coil of a magnetic resonance WPT system for miniaturized biomedical implants was proposed, which can improve the efficiency in the various position of a 9-mm diameter receiver coil. However, the BS-Tx coil was only considered the flowed current driven in the same direction in each loop, leading to the same direction of the magnetic field vectors. The opposite direction of the magnetic field vectors should take into account to analyze sufficiently the phenomenon of the proposed coil. Two prototypes of BS-Tx coil are interpreted by modifying the driven current direction. A 9-mm diameter helical receiving (Rx) coil is designed as an implanted device to receive the transfer energy from the Tx coil. Furthermore, an impedance matching network including a pair of series and parallel capacitors was designed without the method for maximized efficiency in [21]. In this paper, we present a method for extracting the optimal capacitor values to achieve the maximal PTE. With the optimal method, the PTE can be improved several percents in the same conditions. Furthermore, the PTE through the real pork tissue is validated for a practical system to verify the effect of biological tissue on the magnetic resonant WPT system in biomedical implants. Finally, a real-case biomedical scenario is proposed to present the feasibility of the proposed BS-Tx prototypes. The specific absorption rate (SAR) value is simulated to verify the safety regulations in the human body for a hypothetical context of retinal prosthesis application.

This paper is organized as follows. The proposed BS-Tx coil is described and optimized by verifying its shape with the magnetic field evaluation in Section II. The transfer efficiency is also analyzed with the WPT system's characteristic. In Section III, the BS-Tx and Rx coils are fabricated and measured. The measured results are compared with the simulation results and the previous researches. The PTE of the system through the real biological tissue is also presented in this Section. Finally, in Section IV, the BS-Tx WPT system for retinal prosthesis application is demonstrated as a hypothetical context with the SAR verification for the safety constraints.

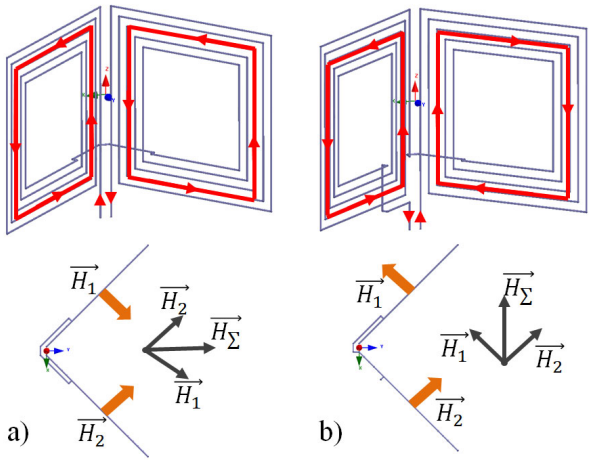

FIGURE 1. Proposed BS-Tx coil structure with its current direction and magnetic field vectors; a) SCSM coil; b) OCOM coil.

II. BIOMEDICAL IMPLANT WPT SYSTEM ANALYSIS

A. BUTTERFLY-SHAPED TRANSMITTING COIL PROTOTYPES

In general, a conventional WPT system requires an accurate alignment between the Tx and Rx coils since a slight misalignment would severely decrease the PTE. A coil with different geometries is designed to modify the magnetic field; this modification of the field leads to a coupling supplement in a misalignment position of the system. The purpose of the system is to have a relatively strong coupled magnetic field between Tx and Rx coils. The topologies of the BS-Tx coil are illustrated in Fig. 1. The BS-Tx coil consists of two spiral coils, which are supplied by an only single power source. The coil is constructed by a 0.5-mm radius Litz-wire with 5 turns for each loop. The dimension of each spiral coil is 10 cm by 10 cm. The WPT system is designed to work at a frequency of 13.56-MHz band that is the most suitable frequency for biomedical implants system [22]. With this operating frequency, the wavelength of the current is much larger than the coil dimension. Therefore, we can assume that the driven current in each coil of the BS-Tx coil is identical and in phase.

In this paper, we consider two prototypes of the BS-Tx coil with the same-current, same-magnetic field direction (SCSM) and the opposite-current, opposite-magnetic field direction (OCOM) on the coordinate axis $\vec{OY}$, as shown in Fig. 1. In Fig. 1(a), the SCSM coil is constructed so that the driven current flows in the same direction on each loop of the coil. In the first half-period, the current flows in the clockwise direction in the both of the loops. Therefore, applying the Screw-law, the magnetic field vectors $\vec{H}_1$, $\vec{H}_2$ are generated by the driven current perpendicular to each loop and the same sign of the direction, as depicted in Fig. 1(a). The total magnetic vector $\vec{H}_\Sigma$ of the BS-Tx coil is the sum of the magnetic

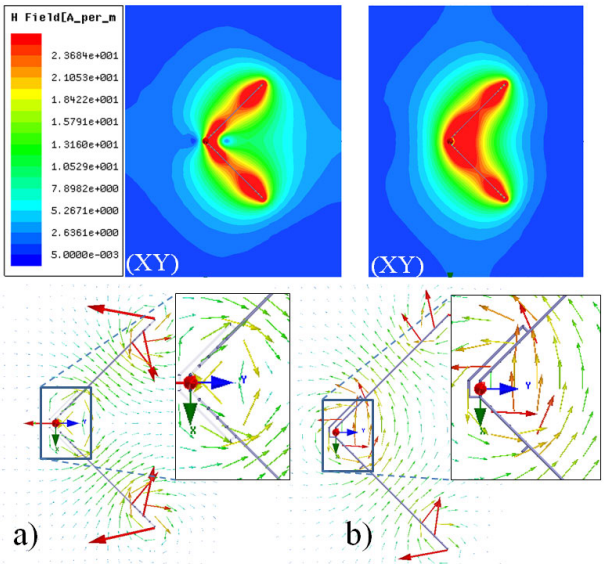

FIGURE 2. Magnetic field magnitude and vector simulation of the BS-Tx coils; a) SCSM coil; b) OCOM coil.

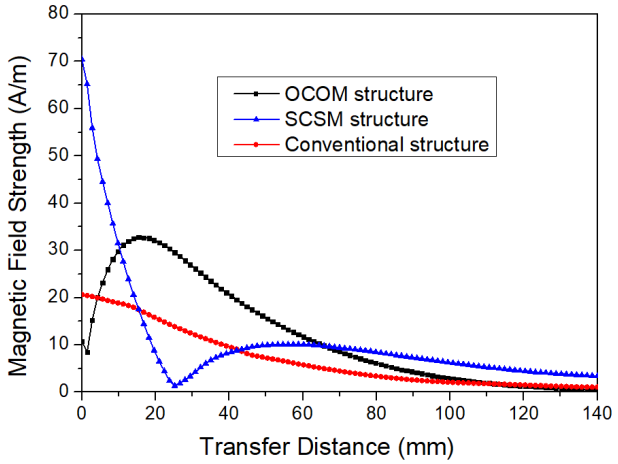

FIGURE 3. Comparison of the H-fields between two BS-Tx coil prototypes and a conventional coil depending on the transfer distance.

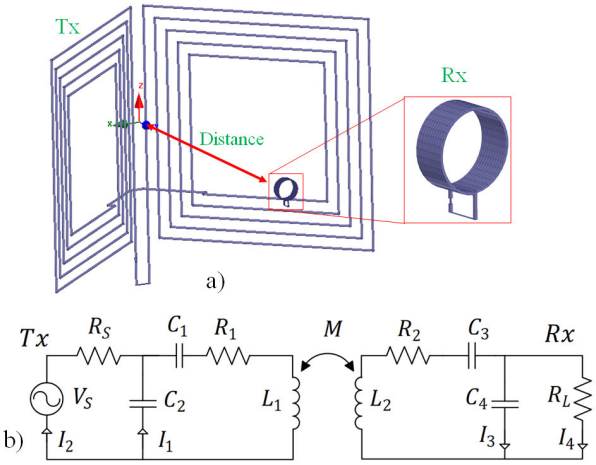

FIGURE 4. a) Proposed WPT system with the Rx coil that is placed at a distance from the origin of the coordinate system; b) equivalent circuit model of the resonant coupling two-coil system, which is composed of lumped components. The resonators are linked by mutual inductance.

vector of each loop. In this topology, the $\vec{H}_\Sigma$ vector is focused and forwarded to the further receiving area. It is obvious to predict that the magnetic field is concentrated by the component magnetic fields, leading to the longer transferred energy to the receiver. Another topology of the BS-Tx coil is OCOM coil that is shown in Fig. 1(b). The OCOM coil is constructed with the same size and shape to the SCSM coil. However, the current flows opposite direction on each loop conducive to the different signs of the generated magnetic field vectors. The total magnetic vector $\vec{H}_\Sigma$ has a trend to direct back and forth between two loops. It is observed that the magnetic field strength in the near receiving area is improved significantly.

Based on the principle of the structure analyzed above, we simulated the Tx prototypes to evaluate the magnetic fields. The magnetic field magnitude and vector of the BS-Tx coils are illustrated in Fig. 2. The SCSM structure presents the magnetic field synthesis that is focused and forwarded to the receiving area leading to the significant enhancement in the further transfer distance. Furthermore, the magnetic field at the receiving area is collected by the more magnetic field vectors of each loop with the same direction, that can compensate the field magnitude in the misalignment conditions. In contrasts, the OCOM structure shows an extremely strong magnetic field in the near area and gradual decrease along the coordinate axis. The magnetic vector of this coil has a good agreement with the above analysis, that directs back and forth between two loops, as demonstrated in Fig. 2(b).

Fig. 3 shows a comparison of the H-fields between two Tx coil prototypes and a conventional coil, which are the same size and number of turn, according to the charging distance. In the near charging area, the OCOM structure generates a dominate magnetic field compared to the SCSM structure around 6 cm distance from the origin of the coordinate system. However, the SCSM structure can maintain significantly the strength of the field in the farther distance. Both proposed prototypes have a stronger magnetic field strength than the conventional coil in the interested receiving area. Therefore, the specific application for biomedical implants of each prototype can be used based on the distance from the implanted devices to the Tx coil.

B. CIRCUIT MODEL AND SYSTEM ANALYSIS

In the biomedical implant system, the Rx coil size is minimized because of the limited volume of the implanted devices. A helical Rx coil is designed as small as 9-mm diameter with 10 turns, as shown in Fig. 4(a). The Rx coil is made with small copper wire with a diameter of 0.3 mm. Fig. 4(b) shows the equivalent circuit model of the proposed WPT system to analyze the transfer efficiency. The schematic is composed of two resonant circuits corresponding to the Tx and Rx coils. The Tx and Rx coils can be modeled as

inductors (L_1, L_2) with parasitic resistances (R_1, R_2). Series capacitors (C_1, C_3) and parallel capacitors (C_2, C_4) are added to control the resonant frequency and reduce the reactance of the Tx and Rx coils. By using a series capacitor and a shunt capacitor, the coil impedance can be matched with almost load impedance [23]. In this paper, a method to extract the values of C_1, C_2, C_3, C_4 is proposed to obtain the optimal PTE of the system. The PTE is calculated according to the $|S_{21}|$ by PTE $= |S_{21}|^2 \times 100(\%)$. The equivalent $|S_{21}|$ scattering parameter can be calculated by

$$|S_{21}| = 2\left|\frac{V_L}{V_S}\right|\sqrt{\frac{R_S}{R_L}} \tag{1}$$

where the transfer function is

$$\begin{aligned}\frac{V_L}{V_S} &= \frac{j\omega k_\varphi \sqrt{L_1 L_2} R_L}{\omega^4 k_\varphi^2 L_1 L_2 C_2 C_4 R_S R_L - j\omega^3 k_\varphi^2 L_1 L_2 (C_2 R_S + C_4 R_L)} \\ &\quad - \omega^2 (k_\varphi^2 L_1 L_2 - C_2 C_4 R_S R_L Z_1 Z_2) - j\omega [C_2 R_S Z_1 (R_L \\ &\quad + Z_2) + C_4 R_L Z_2 (R_S + Z_1)] - (R_S + Z_1)(R_L + Z_2). \\ &= \frac{1}{f(C_1, C_2, C_3, C_4)}. \end{aligned} \tag{2}$$

The function $f(C_1, C_2, C_3, C_4)$ is the non-linear function of arguments C_1, C_2, C_3 and C_4. With given values ω and k_φ, the absolute of transmission parameter $|S_{21}|$ can be maximized by the optimal coefficients C_1, C_2, C_3, C_4 which are extracted by solving the optimization problem formulated as

$$\begin{aligned} &\min_{C_1, C_2, C_3, C_4} |f(C_1, C_2, C_3, C_4)| \\ &\text{subject to } C_i > 0 \quad \forall i \in 1 \ldots 4 \end{aligned} \tag{3}$$

Let $g(C_1, C_2, C_3, C_4) = |f(C_1, C_2, C_3, C_4)|$, the optimization problem (3) is converted into a new form as

$$\begin{aligned} &\min_{C_1, C_2, C_3, C_4} g(C_1, C_2, C_3, C_4) \\ &\text{subject to } |C_1 + C_2 + C_3 + C_4| \\ &\qquad = |C_1| + |C_2| + |C_3| + |C_4|. \end{aligned} \tag{4}$$

By using the method of Lagrange multipliers, the optimal solution of (4) can be obtained by solving the unconstrained optimization problem as follows:

$$\min_{C_1, C_2, C_3, C_4} \mathcal{K} = g(C_1, C_2, C_3, C_4) + h(C_1, C_2, C_3, C_4, \lambda) \tag{5}$$

where

$$\begin{aligned} h(C_1, C_2, C_3, C_4, \lambda) = \lambda\big(&|C_1| + |C_2| + |C_3| + |C_4| \\ &- |C_1 + C_2 + C_3 + C_4|\big) \end{aligned} \tag{6}$$

λ is the positive Largrange multiplier. The optimal solution of (5) is found by iteration. At each iteration, (C_i) and λ are updated simultaneously as

$$(C_i)_{k+1} = (C_i)_k - \mu g_{C_i}, \tag{7}$$

$$\lambda_{k+1} = \lambda_k - \mu g_\lambda. \tag{8}$$

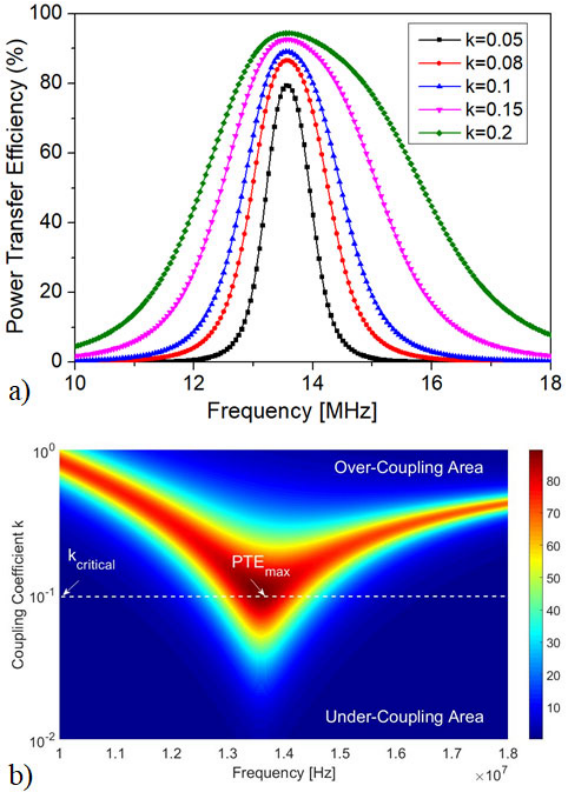

FIGURE 5. a) Dependence between PTE and coupling coefficient k values with the optimal capacitors; b) PTE as a function of frequency and coupling coefficient k with an optimal set of capacitors corresponding to the $k_{critical}$ of 0.1.

where μ is a small step, $g_{C_i} = \nabla_{C_i}\mathcal{K}$ and $g_\lambda = \nabla_\lambda \mathcal{K}$ are the gradients which are given by

$$\nabla_{C_i}\mathcal{K} = \nabla_{C_i} g + \nabla_{C_i} h, \tag{9}$$

$$\nabla_\lambda \mathcal{K} = \nabla_\lambda h. \tag{10}$$

Then, these optimal coefficients C_i are used for calculating the power transfer efficiency PTE. Fig. 5(a) shows the maximal PTE depending on the coupling coefficient k with the optimal capacitors C_1, C_2, C_3, C_4. For each value of k, we can find a set of value of capacitors so that the PTE is the highest, or the k is the critical $k_{critical}$ [24]. It is obvious that the lower value of k is, the lower maximal PTE can be obtained. Fig. 5(b) demonstrates the dependence of the PTE on coupling coefficient k and frequency with the given capacitors. From Fig. 5(b), it is obvious that the coupling coefficient increases followed by frequency splitting. The PTE can reach a peak at the resonant frequency and a critical coupling point $k_{critical}$. When k is greater or less than this point, the delivered power, which is represented by transfer efficiency, falls rapidly at the operating frequency. When k is small, it corresponds to a case in which the system is under-coupled; when k is higher than the critical coupling point, the system is over-coupled, and operating at either resonance will result in maximum power transfer. In the biomedical implant WPT system, the coupling coefficient k value is

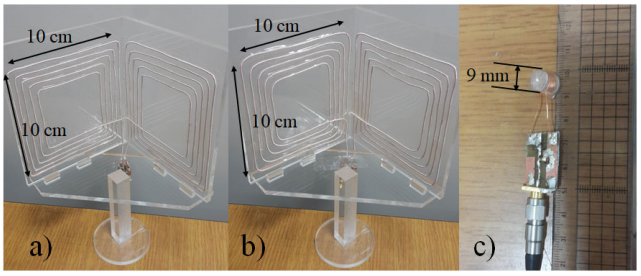

FIGURE 6. Fabricated BS-Tx coil prototypes; a) SCSM coil; b) OCOM coil; c) 9-mm diameter helical Rx coil.

TABLE 1. Extracted component values of the Tx and Rx.

Tx			Rx	
Parameter	Value		Parameter	Value
	SCSM	OCOM		
R_1	24.01 Ω	20.2 Ω	R_2	1.06 Ω
L_1	11.65 uH	12.8 uH	L_2	0.98 uH
C_1	15 pF	16 pF	C_3	157 pF
C_2	230 pF	270 pF	C_4	1.5 nF

often small because of the minimized Rx coil size leading to the weak mutual inductance between the Tx and Rx coils. Therefore, the maximal PTE is also small despite optimal capacitors.

III. FABRICATION AND EXPERIMENTAL VERIFICATION OF THE WPT SYSTEM

A. FABRICATION OF THE BS-TX COILS

To verify the theoretical analysis, the proposed WPT system was fabricated and measured to validate the performance through the PTE value. The BS-Tx coil was constructed using a long Litz-wire with a radius of 0.5 mm for both prototypes of BS-Tx coils, as shown in Fig. 6(a)-(b). The 9-mm diameter helical Rx coil was wound using small solid copper wire with a diameter of 0.3 mm, as illustrated in Fig. 6(c). First, to determine the working frequency, each coil was tested separately with a Protek A333 network analyzer. The detailed values of the lumped elements and extracted parasitic components of the Tx and Rx coils are listed in Table 1. Based on the optimal method analyzed in section II.B, the set of capacitors are obtained for the maximal PTE, as shown in Table 1. The calculated values of capacitors are slightly different from the experiment values because of the fabrication tolerances.

B. MEASUREMENT AND COMPARISON OF MUTUAL INDUCTANCE BETWEEN THE TX AND RX COILS

Once the Tx and Rx parameters and their working frequencies were established, the Rx coil was displaced in a range from 5 cm to 14 cm at a distance from the origin of the coordinate system. The configuration of the resonant coupling system fabrication to confirm the simulation results using the network analyzer is shown in Fig. 7. The mutual inductances between the Tx and Rx coils are measured for both BS-Tx

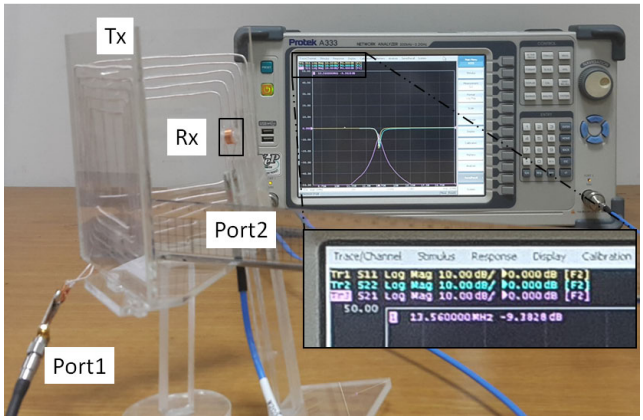

FIGURE 7. Measurement configuration for the resonant coupling system. Ports 1 and 2 of the Network Analyzer Protek A333 are connected to the Tx and Rx coils, respectively.

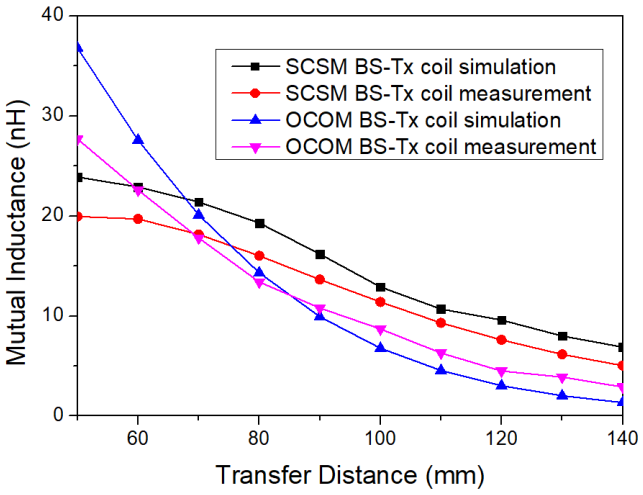

FIGURE 8. Dependence between the mutual inductance and transfer distance of the proposed BS-Tx coil prototypes.

coil prototypes. A comparison of the mutual inductance between simulated and measured results are plotted in Fig. 8. The mutual inductance of the OCOM coil is much higher than the one of the SCSM coil in the near area around 5 cm to 8 cm, then it is rapidly decreased in the further distance. The mutual inductance of the SCSM coil can be kept unchanged through the wide range of the distance. There is a good agreement between the simulated and measured results. Measured results are slightly lower than others because of the fabricated tolerance.

C. MEASUREMENT THE PTE OF THE WPT SYSTEM

The S-parameters were measured using a network analyzer at the resonant frequency of 13.56 MHz, with the transfer distance from 5 cm to 14 cm between the Tx and Rx coils. The return loss values of the Tx and Rx coils at the operating frequency were insignificant due to a good match with the resonant circuits. The PTE was calculated from the square of the S-parameter $|S_{21}|$ as illustrated in Fig. 9. The OCOM

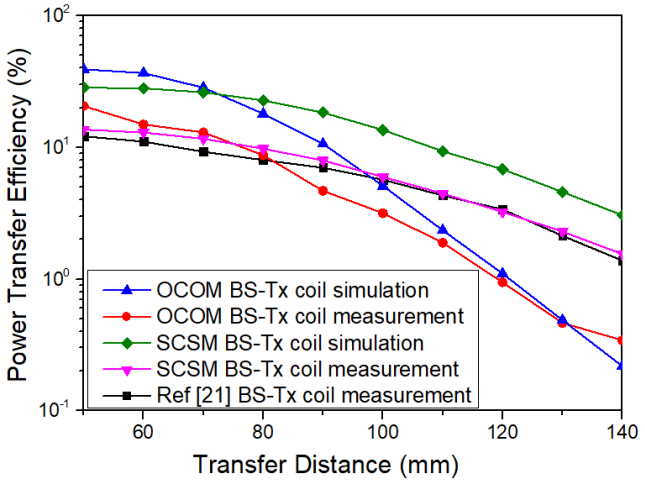

FIGURE 9. Comparison of the proposed BS-Tx coil prototypes' PTE and reference coil according to the transfer distance.

BS-Tx structure presents a high efficiency in a near receiving area from the Tx coil around 5 cm to 8 cm, however, the PTE is rapidly decreased when the Rx coil moved further from the Tx coil. In contrast, the SCSM BS-Tx coil shows the maintained efficiency and slow degradation despite the distance. It is easy to observe that the OCOM BS-Tx structure has the same characteristic with a conventional coil structure, but it can achieve a better performance in a near receiving area compared to the conventional coil. Besides, the SCSM BS-Tx coil has an advantage of maintaining efficiency along the moving path of the Rx coil. In this paper, a method to obtain the maximized PTE was proposed by the optimal pair of capacitors for each Tx and Rx coils. Therefore, the PTE of the BS-Tx structure is higher than the one in [21] without the optimal method, as demonstrated in Fig. 9.

To verify the performance of the system in the angle and axial misalignment, the Rx coil was varied from -6 cm to 6 cm and 0^o to 90^o at a distance of 7 cm. In Fig. 10(a), the PTE of the SCSM coil is insignificantly decreased and kept unchanged around 10 % despite rotation of the Rx coil to 70^o at a distance of 7 cm. Similarly, when the Rx coil is moved from -6 cm to 6 cm at a distance of 7 cm, the PTE of the SCSM system is also sustained in a wide moving range, as illustrated in Fig. 10(b). The OCOM coil exhibits the same characteristics of the conventional coil with better performance in the near receiving area. Therefore, the proposed BS-Tx coil can be significantly improved and overcome the PTE degradation with variations of the Rx coil position.

D. MEASUREMENT THE RECEIVED POWER OF THE WPT SYSTEM

The WPT system can be measured to verify the received power dependence on the input power. A signal generator (Agilent E4436B) was used to supply the input power to the Tx coil, while a power meter was used to measure the delivered power of the Rx coil by a spectrum analyzer (Agilent 85665EC). The experimental setup of the WPT system is

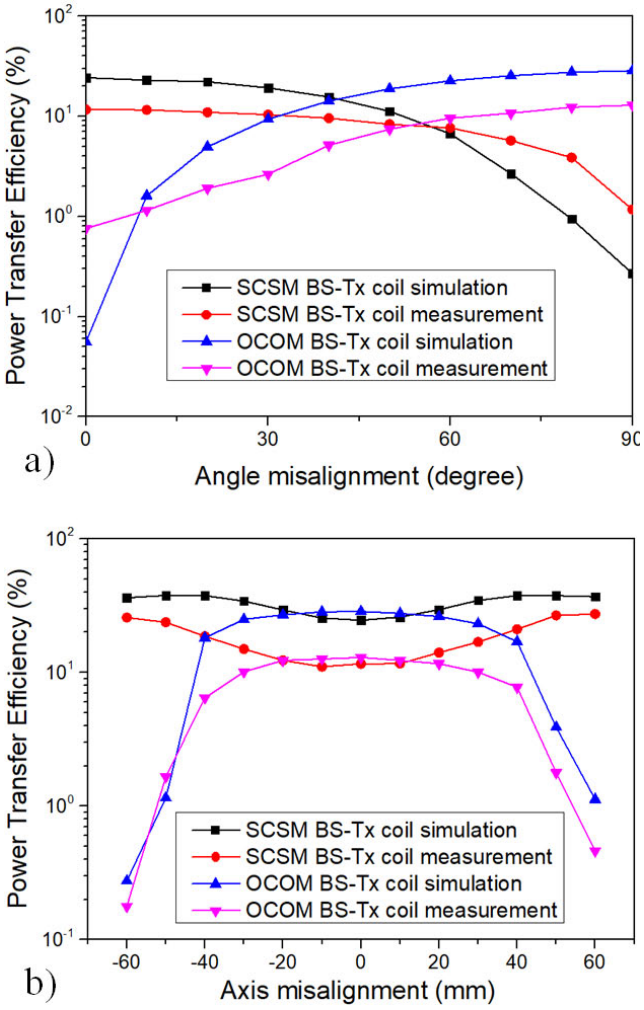

FIGURE 10. Measured performance of the proposed systems with a comparison to simulation results; a) PTE versus angle misalignment from 0^o to 90^o at a distance of 7 cm; c) PTE versus axial misalignment from -6 cm to 6 cm at a distance of 7 cm.

shown in Fig. 11. In order to validate the delivered power, the induced power to the Tx coil was changed from 10 mW to 120 mW. The received power of the Rx coil was measured corresponding to various input power. The PTE and received power dependence on the input power is illustrated in Fig. 12. The received power is increased when the induced power to the Tx coil is increased for both BS-Tx prototypes. However, the OCOM coil has a trend to receive a slightly higher power compared to the SCSM coil.

E. EFFECT OF BIOLOGICAL TISSUE

A current can be induced through a conducting material by a time-variant magnetic flux caused the effect on the wireless power performance. Fortunately, the conductivity of the real tissue is significantly small compared to metal [19]. Therefore, it is expected that the biological tissue does not affect the transfer efficiency in biomedical implants. Fig. 13 shows the experimental setup to verify the effect of real tissue on the PTE using pork tissue. A real human head model is used to

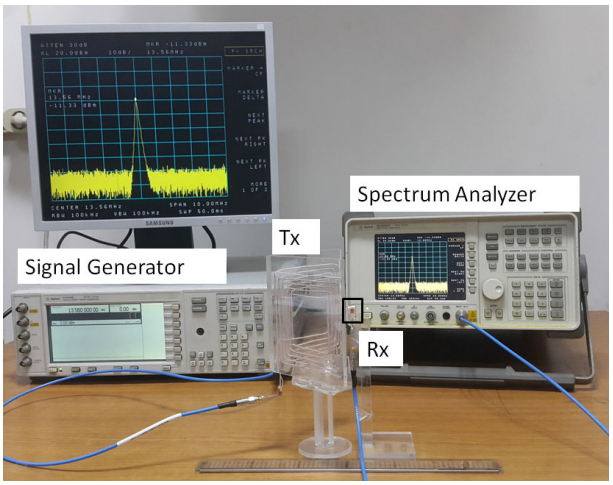

FIGURE 11. Experimental setup of the WPT system for measurement of the dependence of the delivered power on the induced power.

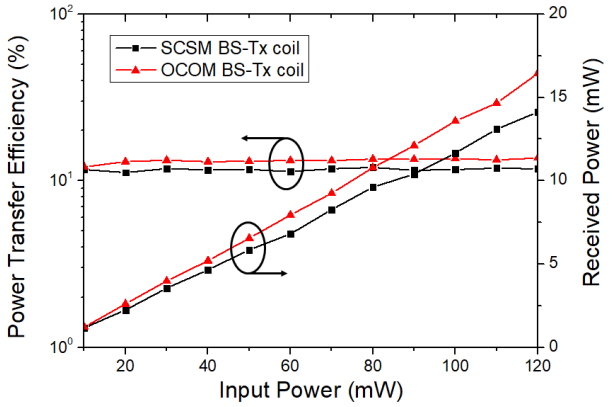

FIGURE 12. Dependence between PTE, received power and input power supplied to the BS-Tx coils.

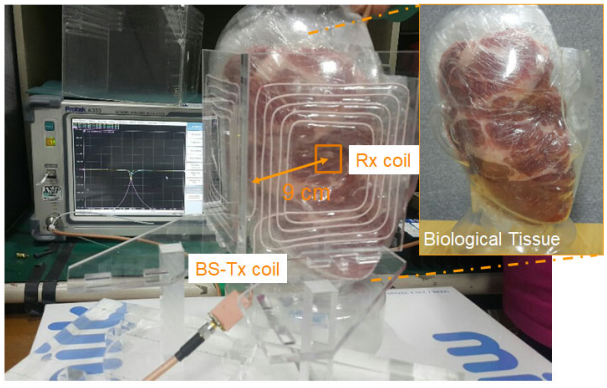

FIGURE 13. Experimental configuration for real tissue verification to the PTE value.

contain the pork chop for experimental configuration. The Rx coil is placed at the eyeball region with a distance of around 9 cm from the origin of the coordinate system of BS-Tx coil. Fig. 14 illustrates the experimental PTE values of SCSM and OCOM BS-Tx coils with and without the pork tissue.

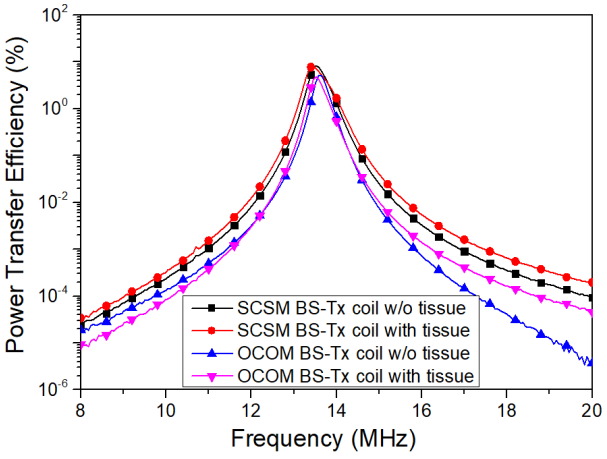

FIGURE 14. Comparison of PTE values of BS-Tx prototypes with and without the pork tissue.

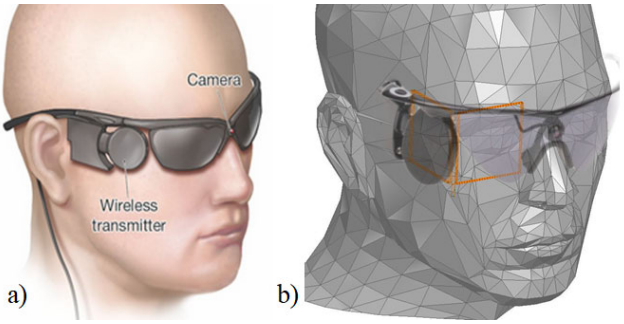

FIGURE 15. a) ARGUS II Retinal Prosthesis; b) Proposed BS-Tx coil embedded in a glasses frame.

It is obvious that the peak efficiencies of the WPT system are insignificantly changed when the pork tissue is inserted between the Tx and Rx coils.

IV. BS-TX WPT SYSTEM FOR RETINAL PROSTHESIS

Based on the specific characteristic of BS-Tx prototypes, the hypothetical context of a biomedical application is proposed. The SCSM BS-Tx coil shows the maintained efficiency and slow degradation despite the distance, while the OCOM coil exhibits the same characteristics of the conventional coil with better performance in the near receiving area. Both of the proposed BS-Tx prototypes can be significantly improved and overcome the PTE degradation with variations of the Rx coil position. In this paper, we validate a real-case biomedical scenario for the proposed technique in retinal prosthesis application because the rotated eyeball leads to the coil misalignment.

A. HYPOTHETICAL CONTEXT OF A BIOMEDICAL APPLICATION

Artificial vision is considered retinitis pigmentosa (RP) patients with total blindness or fading tunnel vision. Fig. 15(a) shows the ARGUS II retinal prosthesis system developed by the Second Sight Medical Products, which is

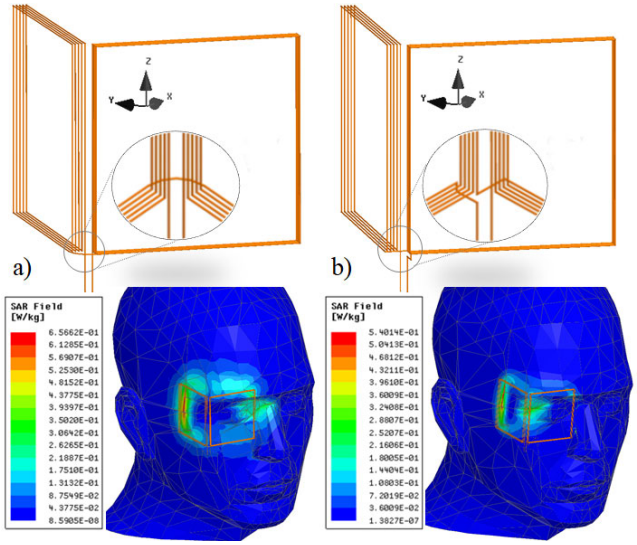

FIGURE 16. SAR simulation for the proposed BS-Tx prototypes; a) SCSM BS-Tx coil; b) OCOM BS-Tx coil.

an epiretinal device approved for implantation in patients with end-stage RP [25]. The external equipment includes the glasses, a video processing unit and a cable. The glasses include a miniature video camera and a Tx coil that transmits the data along with power and stimulation command to the implant [26], [27]. The transmitting module includes a single Tx coil, that must be near close to the internal coil. In this paper, the BS-Tx prototypes are proposed to embedded into the glasses as shown in Fig. 15(b). One loop of the BS-Tx coil is placed at the same position with the ARGUS II's transmitter coil, while the other loop is attached in the glasses frame. With this configuration of the transmitting module, the feature of the BS-Tx coil is presented with the complete characteristics to overcome the PTE degradation in conventional retinal prosthesis system.

B. SPECIFIC ABSORPTION RATE (SAR) VERIFICATION

The electromagnetic field absorption in the human body is certified by the SAR value, which represents the absorbed energy in the human body. The SAR is set a restriction of 2W/kg for head and trunk at a frequency range of 100 kHz to 300 GHz. The higher SAR value is, the more harmful the WPT system induces. In this paper, the ANSYS HFSS simulation tool is used to validate the safety of the system by SAR value. Fig. 16 shows the 3-D graph of the WPT system to indicate the SAR simulation for both of BS-Tx prototypes, which are slightly modified to be suitable with the retinal prosthesis application. The coils are both constructed by the small copper wire with a diameter of 0.3 mm. The dimension of each loop is 5 cm by 5 cm corresponding to the dimension of the glasses frame. The SAR values are approximately 0.65 W/kg and 0.54 W/kg averaging over 1-g of tissue corresponding to the SCSM and OCOM BS-Tx coil, respectively. The SAR values are much smaller than the limitation restriction for the head/trunk, that are satisfied the human safety regulations.

V. CONCLUSION

In this paper, we presented two BS-Tx coil prototypes of a magnetic resonant WPT system with a 9-mm diameter Rx coil for biomedical implants. It was shown that the proposed Tx coils can significantly improve the PTE of the system in the misalignment tolerance of the Rx coil, such as transfer distance, angle and axis misalignment. The optimal method for extracting capacitors was proposed to obtain the maximal PTE. The dependences between PTE and distance, angle and axis misalignment were investigated to verify the performance of the WPT system. The BS-Tx prototypes have been validated the efficiency through the biological tissue in the retinal prosthesis application to present the feasibility of the proposed system. The SAR value is also verified to confirm the safety of the proposed system for the feasibility in a human body.

REFERENCES

[1] M. Meng and M. Kiani, "A hybrid inductive-ultrasonic link for wireless power transmission to millimeter-sized biomedical implants," *IEEE Trans. Circuits Syst. II, Exp. Briefs*, vol. 64, no. 10, pp. 1137–1141, Oct. 2017.

[2] M. Zargham and P. G. Gulak, "Maximum achievable efficiency in near-field coupled power-transfer systems," *Trans. Biomed. Circuits Syst.*, vol. 6, no. 3, pp. 228–245, Jan. 2012.

[3] A. K. RamRakhyani, S. Mirabbasi, and M. Chiao, "Design and optimization of resonance-based efficient wireless power delivery systems for biomedical implants," *Trans. Biomed. Circuits Syst.*, vol. 5, no. 1, pp. 48–63, Feb. 2011.

[4] H.-J. Kim, H. Hirayama, S. Kim, K. J. Han, R. Zhang, and J.-W. Choi, "Review of near-field wireless power and communication for biomedical applications," *IEEE Access*, vol. 5, pp. 21264–21285, Sep. 2017.

[5] G. Wang, P. Wang, Y. Tang, and W. Liu, "Analysis of dual band power and data telemetry for biomedical implants," *Trans. Biomed. Circuits Syst.*, vol. 6, no. 3, pp. 208–215, Jun. 2012.

[6] H. Jiang, J. Zhang, D. Lan, K. K. Chao, S. Liou, H. Shahnasser, R. Fechter, S. Hirose, M. Harrison, and S. Roy, "A low-frequency versatile wireless power transfer technology for biomedical implants," *IEEE Trans. Biomed. Circuits Syst.*, vol. 7, no. 4, pp. 526–535, Aug. 2013.

[7] S. Stoecklin, A. Yousaf, T. Volk, and L. Reindl, "Efficient wireless powering of biomedical sensor systems for multichannel brain implants," *IEEE Trans. Instrum. Meas.*, vol. 65, no. 4, pp. 754–764, Apr. 2016.

[8] A. S. Y. Poon, S. O'Driscoll, and T. H. Meng, "Optimal frequency for wireless power transmission into dispersive tissue," *IEEE Trans. Antennas Propag.*, vol. 58, no. 5, pp. 1739–1750, May 2010.

[9] S. Kim, J. S. Ho, and A. S. Y. Poon, "Wireless power transfer to miniature implants: Transmitter optimization," *IEEE Trans. Antennas Propag.*, vol. 60, no. 10, pp. 4838–4845, Oct. 2012.

[10] M. Ma and A. S. Y. Poon, "Midfield wireless power transfer for bioelectronics," *IEEE Circuits Syst. Mag.*, vol. 15, pp. 54–60, 2nd Quart., 2015.

[11] A. Rajagopalan, A. K. RamRakhyani, D. Schurig, and G. Lazzi, "Improving power transfer efficiency of a short-range telemetry system using compact metamaterials," *IEEE Trans. Microw. Theory Techn.*, vol. 62, no. 4, pp. 947–955, Apr. 2014.

[12] D. Ahn and M. Ghovanloo, "Optimal design of wireless power transmission links for millimeter-sized biomedical implants," *IEEE Trans. Biomed. Circuits Syst.*, vol. 10, no. 1, pp. 125–137, Feb. 2016.

[13] X. Li, C.-Y. Tsui, and W.-H. Ki, "A 13.56 MHz wireless power transfer system with reconfigurable resonant regulating rectifier and wireless power control for implantable medical devices," *IEEE J. Solid-State Circuits*, vol. 50, no. 4, pp. 978–989, Apr. 2015.

[14] H. Lee, R. V. Bellamkonda, W. Sun, and M. E. Levenston, "Biomechanical analysis of silicon microelectrode-induced strain in the brain," *J. Neural Eng.*, vol. 2, no. 4, pp. 81–89, 2005.

[15] G. McConnell, H. Rees, A. Levey, C. Gutekunst, R. Gross, and R. Bellamkonda, "Implanted neural electrodes cause chronic, local inflammation that is correlated with local neurodegeneration," *J. Neural Eng.*, vol. 6, Oct. 2009, Art. no. 056003.

[16] L. Karumbaiah, T. Saxena, D. Carlson, K. Patil, R. Patkar, E. A. Gaupp, M. Betancur, G. B. Stanley, L. Carin, and R. V. Bellamkonda, "Relationship between intracortical electrode design and chronic recording function," *Biomaterials*, vol. 34, no. 33, pp. 8061–8074, Nov. 2013.
[17] W. Biederman, D. J. Yeager, N. Narevsky, A. C. Koralek, J. M. Carmena, E. Alon, and J. M. Rabaey, "A fully-integrated, miniaturized (0.125 mm^2) 10.5 μW wireless neural sensor," *IEEE J. Solid-State Circuits*, vol. 48, no. 4, pp. 960–970, Apr. 2013.
[18] W. Wang, S. Hemour, and K. Wu, "Coupled resonance energy transfer over gigahertz frequency range using ceramic filled cavity for medical implanted sensors," *IEEE Trans. Microw. Theory Techn.*, vol. 62, no. 4, pp. 956–964, Apr. 2014.
[19] A. K. RamRakhyani and G. Lazzi, "Multicoil telemetry system for compensation of coil misalignment effects in implantable systems," *IEEE Antennas Wireless Propag. Lett.*, vol. 11, pp. 1675–1678, 2012.
[20] K. Na, H. Jang, H. Ma, and F. Bien, "Tracking optimal efficiency of magnetic resonance wireless power transfer system for biomedical capsule endoscopy," *IEEE Trans. Microw. Theory Techn.*, vol. 63, no. 1, pp. 295–304, Jan. 2015.
[21] N. Ha-Van and C. Seo, "Butterfly-shaped transmitting coil for wireless power transfer system in millimeter-sized biomedical implants," in *Proc. IEEE Wireless Power Transf. Conf.*, Jun. 2018, pp. 1–4.
[22] R.-F. Xue, K.-W. Cheng, and M. Je, "High-efficiency wireless power transfer for biomedical implants by optimal resonant load transformation," *IEEE Trans. Circuits Syst. I, Reg. Papers*, vol. 60, no. 4, pp. 867–874, Apr. 2013.
[23] N. Ha-Van and C. Seo, "Analytical and experimental investigations of omnidirectional wireless power transfer using a cubic transmitter," *IEEE Trans. Ind. Electron.*, vol. 65, no. 2, pp. 1358–1366, Feb. 2018.
[24] A. P. Sample, D. T. Meyer, and J. R. Smith, "Analysis, experimental results, and range adaptation of magnetically coupled resonators for wireless power transfer," *IEEE Trans. Ind. Electron.*, vol. 58, no. 2, pp. 544–554, Feb. 2011.
[25] Y. H.-L. Luo and L. da Cruz, "The argus ii retinal prosthesis system," *Prog. Retinal Eye Res.*, vol. 50, pp. 89–107, Jan. 2016.
[26] H. C. Stronks and G. Dagnelie, "The functional performance of the Argus II retinal prosthesis," *Expert Rev. Med. Devices*, vol. 11, no. 1, pp. 23–30, 2014.
[27] L. Da Cruz, B. F. Coley, J. Dorn, F. Merlini, E. Filley, P. Christopher, F. K. Chen, V. Wuyyuru, J. Sahel, P. Stanga, M. Humayun, R. J. Greenberg, and G. Dagnelie, "The Argus II epiretinal prosthesis system allows letter and word reading and long-term function in patients with profound vision loss," *Brit. J. Ophthalmol.*, vol. 97, no. 5, pp. 632–636, Feb. 2013.

NAM HA-VAN (M'14) received the B.S. degree from the School of Electronics and Telecommunications, Hanoi University of Science and Technology, Hanoi, Vietnam, in 2012, and the Ph.D. degree in information and telecommunication engineering from Soongsil University, Seoul, South Korea, in 2019, where he is currently a Postdoctoral Researcher with the Soongsil University Foundation of University-Industry Cooperation.

His current research interests include free-positioning wireless power transfer, wireless power transfer in biomedical implants, metamaterials, power amplifiers, phased array antenna, and energy harvesting system.

CHULHUN SEO (M'97–SM'14) received the B.S., M.S., and Ph.D. degrees from Seoul National University, Seoul, South Korea, in 1983, 1985, and 1993, respectively.

From 1993 to 1995, he was with the Massachusetts Institute of Technology (MIT), Cambridge, MA, USA, as a Technical Staff Member. From 1993 to 1997, he was with Soongsil University, Seoul, Korea, as an Assistant Professor. From 1999 to 2001, he was with MIT, as a Visiting Professor. From 1997 to 2004, he was with Soongsil University, as an Associate Professor, where he has been a Professor of electronic engineering, since 2004. He was the IEEE MTT Korea Chapter Chairman, from 2011 to 2014. He is the President of the Korean Institute of Electromagnetic Engineering and Science (KIEES) and the Dean of the Informations and Telecommunications College, Soongsil University. He is the Director of the Wireless Power Transfer Research Center supported by the Korea Government Ministry of Trade, Industry, and Energy, and the Director of Metamaterials Research Center, supported by the Basic Research Laboratories (BRL) through NRF Grant funded by the MSIP. His research interests include wireless communication technologies, RF power amplifiers, and wireless power transfer using metamaterials.